THEORETICAL DFT INTERPRETATION OF INFRARED SPECTRA OF BIOLOGICALLY ACTIVE ARABINOGALACTAN SULPHATED DERIVATIVES

Aleksandr S. Kazachenko*[1] 0000-0002-3121-1666**, Felix N. Tomilin[2,3,4]** 0000-0002-3578-6141**, Anastasia A. Pozdnyakova[2], Natalia Yu. Vasilyeva[1,2], Yuriy N. Malyar[1,2]** 0000-0001-9380-0290**, Svetlana A. Kuznetsova[1], and Pavel V. Avramov[5]** 0000-0003-0075-4198

[1]*Institute of Chemistry and Chemical Technology SB RAS, FRC "Krasnoyarsk Science Center SB RAS", 50/24 Akademgorodok, Krasnoyarsk, 660036, Russia*

[2]*Siberian Federal University, 79 Svobodny pr., Krasnoyarsk, 660041, Russia*

[3]*Kirensky Institute of Physics SB RAS, FRC "Krasnoyarsk Science Center SB RAS", 50/38 Akademgorodok, Krasnoyarsk, 660036, Russia*

[4]*National Research Tomsk State University, Lenin Ave. 36, Tomsk 634050, Russia.*

[5]*Department of Chemistry and Green-Nano Materials Research Center, Kyungpook National University, 80 Daehak-ro, Buk-gu, Daegu, 41566, South Korea*

*Corresponding author: Aleksandr S. Kazachenko leo_lion_leo@mail.ru

Abstract

Arabinogalactan (AG) and sulphated arabinogalactans (SAG) which are products of chemical modification of arabinogalactan polysaccharide with anticoagulant properties were studied by experimental infrared (IR) spectroscopy combined with density functional theory simulations. Mutual analythis of experimental and theoretical IR frequencies indicates that the descripancies between experiment and theory is caused by the influence of -OH groups, which led to the energy shift and broadening of the absorption IR bands. It was found that theoretical and experimental spectra correspond well within 3000-4000 cm^{-1} spectral region. Addition of sulphur group in AG structure causes hydroxyl group to become accessible for further sulphation. The difference between experimental and theoretical IR frequencies of sulphated AG derivatives is greater than for the parent arabinogalactan due to increase in the number of possible isomers and conformers.

Keywords: Arabinogalactan; Sulphated arabinogalactan; FTIR-spectra; Molecular structure; Density functional theory

Introduction

The polysaccharide availability in animals, plants, microorganisms and fungi tissues, their low toxicity, bioavailability and biodegradability makes these biopolymers hold promise for drug development. The sulphate group availability in polysaccharides may increase their specific and non-specific binding with a wide range of biologically important proteins. An important role in these interactions is played by both polysaccharide macromolecule structure (Nader et al. 2004) and possibly its conformation in solution (Becker et al. 2007), as well as the biopolymer molecular weight and the density distribution of the negative charge along its chain.

Sulphated polysaccharides are also widespread in nature, such as, in the tissues of animals, plants, fungi and microorganisms. The largest number of plant polysaccharide sulphates is contained in algae (fucans, fucoidans, carrageenans, etc.). There are also numerous plant polysaccharides in marine invertebrates. Besides the functional properties, individual sulphated polysaccharides demonstrate a variety of pharmacological activity (Alban et al. 2002, Desai 2004). These biopolymers exhibit antiviral, antiparasitic, antiproliferative, anticoagulant, antithrombotic anti-atherosclerotic, anti-ulcer, radioprotective etc. activities. Chronologically heparin discovered at the beginning of the last century became the first known anticoagulant (Mestechkina et al. 2010). This natural sulphated linear glucosaminoglycan is produced by the mast cells of some animal tissues. Widespread medical use of the anticoagulant revealed a number of negative side effects and disadvantages like high cost and labour-intensive production. Various sulphated polysaccharides with different structure, molecular weight and pharmacological properties are known as heparinoids of both natural (chondroitin sulphates, other sulphated glycosaminoglycans), and synthetic (dextran sulphates, chitosan sulphates, etc.) origins have distinctive anticoagulant properties (Ma et al. 2010, Huang, Hu et al. 2008, Huang, Wang et al. 2008, Pereira et al. 2002, Drozd et al. 2006). The anticoagulant activity of sulphated polysaccharides directly depends on the sulphation method, which affects the sulphation degree, the nature of the sulphate group arrangement, molecular weight, etc. (Nader et al. 2004, Desai 2004, Drozd et al. 2006, Chaidedgumjorn et al. 2002, Jiao et al. 2011, Huang, Zhang 2010, Zhang et al. 2011, Kostiro et al. 2008).

In particular, the anticoagulant heparinoid class includes sulphated arabinogalactan (SAG), a product of chemical modification of arabinogalactan (AG) polysaccharide (Figure 1) synthesized as a result of complex waste-free processing of Siberian larch wood (*Larix sibirica Ledeb*.). The AG content in wood reaches 15%, which directly indicates huge reserves of raw materials for mass production of promising biologically active substances.

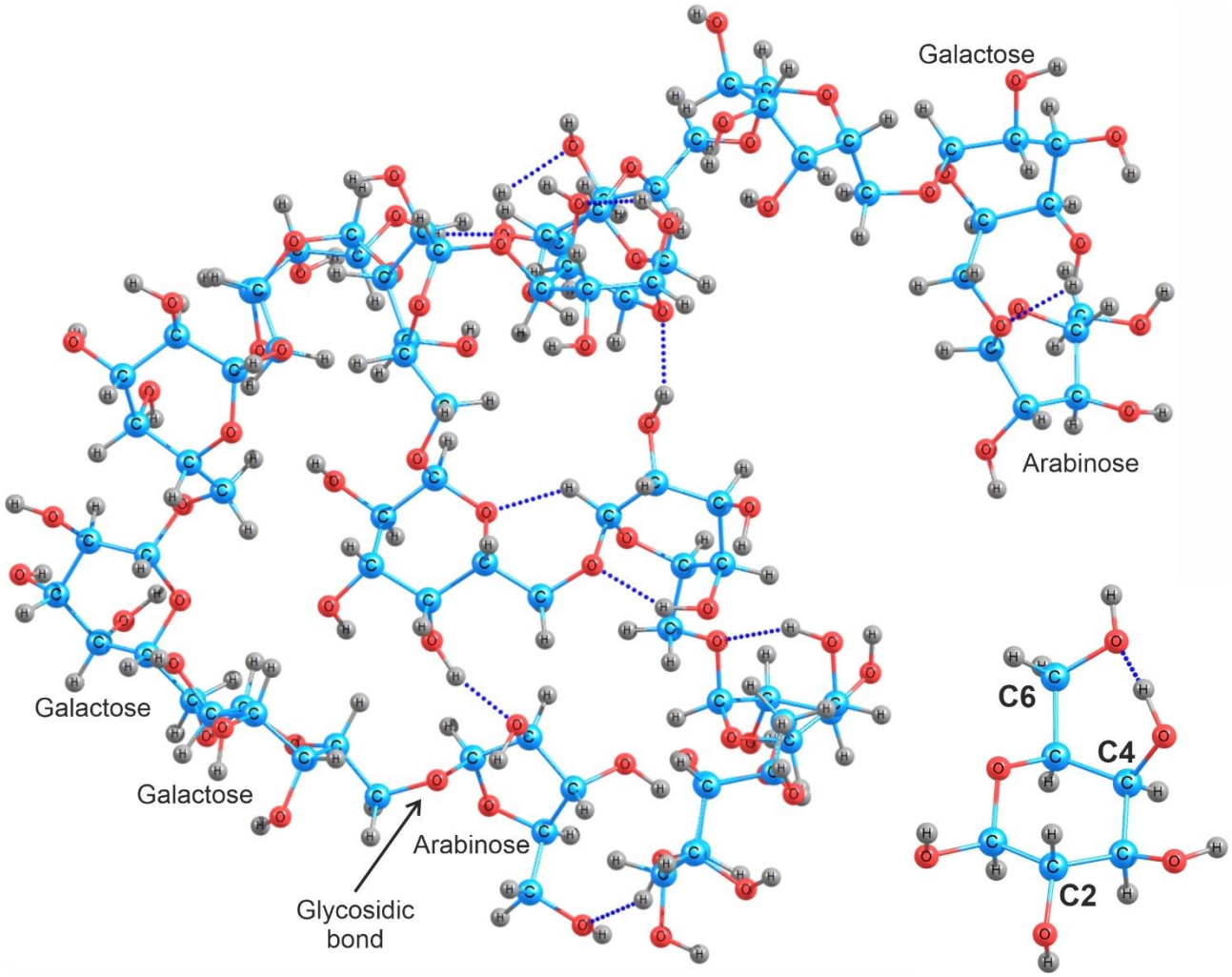

Figure 1. Fragment of the arabinogalactan molecule with marked hydroxyl groups responsible for the occurrence of predominant sulphation. The main chain consists of galactose units linked by glycosidic bonds, and the side chains consist of galactose and arabinose units and separate arabinose units. The blue dotted lines represent intramolecular hydrogen bonds.

Arabinogalactan is a water-soluble polysaccharide with low molecular weight, light coniferous smell and sweet taste (Babkin et al. 2016). It is characterized by a wide range of biological properties like immunobiological, hepatoprotective, antimutagenic, mitogenic, gastroprotective, membranotropic, probiotic, myogenic, lipid-lowering, immunomodulating; it can be used a source of dietary fibre as well (Ermakova et al. 2010).

The main chain of arabinogalactan consists of galactose units linked by β- (1 → 3) glycosidic bonds. The side chains are formed by β- (1 → 6) bonds between galactose and arabinose units, single arabinose units, and of uronic acids, mainly glucuronic acid. It is also acknowledged that AG main chain includes arabinose units as well (Willför ei al. 2004). The ratio of galactose and arabinose units approximately equals to 6:1, with 1/3 of the arabinose units in pyranose form, and 2/3 in furanose one (Babkin et al. 2016, Ermakova et al. 2010). It is expected that AG macromolecules probably exist in a very compact and spherical form (Goellner et al. 2011). For carbohydrates, which include the

arabinogalactan and its sulphate class, there is a correlation of biological activity with molecular structure (Becker et al. 2007, Willför et al. 2004, Goellner et al. 2011, Karacsonyi et al. 1984, Antonova et al. 1984). It was found (Kostiro et al. 2008) that the hydroxyl AG groups, located at C2 and C4 positions in the main galactan chain, and the primary hydroxyl group, located at C6 position of the galactose end units in the main and side chains, are predominantly sulphated. Based on these structural data, the simplest molecular models were developed.

Irregular structure and the coexistence of various functional groups in different substituents positions coupled with tautomeric forms make accurate interpretation of arabinogalactan and its sulphated derivative IR spectra very difficult or almost impossible without clear insight of macromolecule structure and to establish spectral-structural correlations. Combination of the state-of-the-art density functional theory (DFT) and calculations of model molecules with experimental AG and its sulphated derivatives IR spectra makes it possible to overcome these difficulties, to identify spectral band structure, interpret molecular structure like exact positions of sulphate groups and to determine basic biological properties of the macromolecules (Akman 2017, Barsberg 2010, Shanura Fernando et al. 2017, Tran et al. 2018).

Recently, interest in the study of polysaccharides by theoretical methods was increasing (Profant V et al. 2019, Akman F et al. 2020). These methods are based on calculations of spectroscopic characteristics of electron circular dichroism (ECD) (Rudd TR et al. 2009, Matsuo K. et al. 2009), infrared absorption with Fourier transform (FTIR) (Mainreck N. et al. 2009, Akman F et al. 2020, Garnjanagoonchorn W. et al. 2007), Raman spectroscopy (Profant V et al. 2019, Rüther, A et al. 2017, Yaffe NR et al. 2010, Ellis R et al. 2009), spectroscopy nuclear magnetic resonance (Canales A et al. 2017, Klepach T et al. 2015, Gerbst AG et al. 2017, Shklyaev OE et al. 2014, Akman F et al. 2016). The methods allow one to obtain the key properties of a number of polymers (Profant V et al. 2019).

In contrast with artificial polymers, natural polysaccharides have complex and irregular molecular structure determined by uncontrollable conditions of plant growth, which makes advanced interpretation of IR spectra impossible without implementation of DFT theory. The goal of this work is to achieve a detailed interpretation of experimental IR spectra of arabinogalactan and sulphated arabinogalactan by means of state-of-the-art density functional theory (DFT) electronic structure calculations and vibration spectra simulations.

Materials and Methods

Arabinogalactan of Siberian larch wood (*Larix sibirica Ledeb.*) produced by “Khimia drevesiny” (Irkutsk, Russia) under the name of “FibrolarS” was taken as a raw material. The samples with different sulphur contents (3.2; 5.1, 9.4 wt.%) were obtained by sulphating of arabinogalactan using sulphamic

acid-urea complex method (Vasil'eva et al. 2015), which is based on the reaction of sulphamic acid and urea in 1,4-dioxane. IR spectra of arabinogalactan and its sulphation products were phased out using Tensor-27 FT-IR spectrometer (Bruker, Germany) in the wavelength range of 400-4000 cm^{-1}. The spectral information was processed by OPUS code (version 5.0). The solid samples for analysis were prepared as the tablets in a KBr matrix (2 mg of sample/1000 mg of KBr). The absorption band assignment was carried out following the procedure described in Refs. 29, 30.

In contrast with parent AG (Figure 2, a), all SAG samples reveal high-intensity IR bands at 1250-1260 cm^{-1}, assigned to asymmetric stretching vibrations υ_{as}(O=S=O) (Figures 2b, 2c, 2d, and 2e). The absorption IR bands in all SAG samples at 810-815 and 860-870 cm^{-1} are assigned to primary and secondary sulphate groups. The intensities of SAG IR bands at 3420–3440 cm^{-1} and 1370– 1380 cm^{-1} spectral regions, which are assigned to the stretching and planar deformation vibrations of OH groups respectively, were observed to decrease due to substitution of hydroxyls by SO_3 groups. The higher the sulphur content (wt.%), the higher the SAG peak intensities in spectral regions of 1250-1260 cm^{-1} and 810-815 cm^{-1}, which correspond to sulphate group vibrations. In the case of sulphur content of 9.4 wt.% (Figure 2, e), the sulphated arabinogalactan IR spectrum exhibits a more distinct peak at 1463 cm^{-1}, which corresponds to vibrations of -CH_2- bonds, which may relate to the polysaccharide degradation processes under sulphation.

Calculation methods

The electronic structure calculations of AG and SAG molecules as well as corresponding Hessians were performed using DFT theory at B3LYP level of theory and 6-31+G(d) basis set (Lee et al. 1988, Shmidt et al. 1993). All electronic structure calculations were performed using GAMESS package (Stewart 2004). It is well known that B3LYP functional combined with Gaussian basis sets yields a good agreement between calculated parameters of organic compounds and experiment (Curtiss et al. 1997, Curtiss et al. 2005, Tirado-Rives et al. 2008, Fredj et al. 2017). To calculate molecular and electronic structure and theoretical IR spectra, several conformers of arabinogalactan with different hydroxo group arrangement regarding the pyranose cycle of galactose were considered. All electronic structure calculations were performed for closed electronic shells in the singlet state and neutral charge for gas phase since AG and SAG molecules have no regular crystal structure and do not interact with any solvents. KBr powder matrix provides low concentration of AG and SAG molecules which prevents interactions between the organic phase. Composition of arabinogalactan polysaccharide is mostly (by 90%) is determined by galactose structural units, so the molecular models of AG and SAG were developed based on two galactose groups. Following structural data of Ref. 17, structural models of sulphated arabinogalactan with sulphate groups in 2 (SAG-2), 4 (SAG-4), 6 (SAG-6,) and 2, 4 (SAG-

2,4) positions were developed. To consider possible dimerization of the molecules during sample preparation in KBr matrix, structural models of arabinogalactan and sulphated arabinogalactan (SAG-2,4) with chains consist of two galactose, arabinogalactan and sulphated units in 2,4 AG positions were calculated. Theoretical AG and SAG IR spectra were calculated by multiplication of Hessian matrix elements by 0.945 factor, which was obtained by renormalization of theoretical spectrum of pure arabinogalactan in comparison with experimental one. This is a standard procedure since it is known that the standard error in the determination of theoretical intensities of IR spectra is approximately 5-10%, depending on the calculation method. Often 2-params scaling (Palivec et al. 2020) are performed to present IR spectra, but due to the fact that mainly the long-wavelength range was required in this particular study, the uniform scaling was applied. The IR spectra band assignment was carried out based on shape vibration analysis corresponding to the definite frequency and calculated atomic vibration amplitudes.

Results and Discussion

Theoretical and experimental absorption frequencies of chemical bonds in functional groups of arabinogalactan and sulfated arabinogalactan molecules are presented in Tables 1 and 2. The relative errors (RE) of IR frequencies were calculated following the formula $RE=(OF_{exp}-OF_{theor})\cdot 100\%/OF_{exp}$, where OF_{exp} and OFt_{heor} are experimental and theoretical oscillator frequencies, respectively. The discrepancy between theoretical and experimental IR frequencies for arabinogalactan is equal to 7.9% of 3425 cm^{-1} as presented in Table 1. In high-frequency spectral region (2900-3700 cm^{-1}), the frequency absolute errors reach 64-270 cm^{-1}. For middle range frequencies (600-1700 cm^{-1}) the error magnitude becomes smaller and equal to ???. It is shown that the largest relative errors are observed for the oscillation frequencies corresponding to OH-groups, which is probably caused by the great contribution of hydrogen bonds between multiple hydroxyls in arabinogalactan, thereby led to energy shifts and broadening of absorption IR bands.

Table 1 Theoretical (B3LYP/6-31+G (d)) and experimental absorption frequencies of parent arabinogalactane.

Absorption frequency	Oscillation frequency, cm^{-1}		Band assignment *
	Theory	Experiment	
1	650	617	$\delta_{(R\text{-}OH)}$
2	741	773	$\upsilon_{(C\text{-}C)}$, $\delta_{(R\text{-}OH)}$, $\rho_{(CH_2)}$
3	1070	1077	$\delta_{(OH)}$, $\upsilon_{(C\text{-}O)}$, $\rho_{(CH_2)}$
4	1124	1156	$\tau_{(CH_2)}$,$\delta_{(OH)}$, $\upsilon_{(C\text{-}O)}$, $\delta_{(C\text{-}O\text{-}C)}$
5	1285	1258	$\omega_{(CH_2)}$, $\upsilon_{(C\text{-}O)}$, $\delta_{(OH)}$
6	1338	1339	$\delta_{(\text{-}CH\text{-})}$, $\omega_{(CH_2)}$, $\tau_{(CH_2)}$

7	1386	1376	$\delta_{(OH)}$, $\upsilon_{(C-O)}$, $\omega_{(CH_2)}$
8	1410	1418	$\omega_{(CH_2)}$, $\delta_{(OH)}$, $\upsilon_{(C-O)}$, $\upsilon_{(C-C)}$
9	1446	1456	$\delta_{(-CH_2-)}$
10	1597	1629	$\delta_{(OH)}$, $\upsilon_{(C-O)}$
11	2921	2985	$\upsilon_{(CH_2)}$
12	3695	3425	$\upsilon_{(OH)}$

*The following notations are used: ν corresponds to stretching vibration, δ, ρ, ω, τ correspond to bending vibration (scissoring, rocking, wagging, twisting). Corresponding chemical bonds are indicated as subscript indexes in the brackets. Determination of spectral bands according to reference (Babkin et al. 2016)

As it is shown in Figure 2, the SAG-2, SAG-4, SAG-6, SAG-2,4, spectra have similar absorption bands in 0-1700 cm^{-1} region. A significant shift of SAG-2,4 high-intensity OH band, corresponding to the group of smaller values in the area of 2800-3700 cm^{-1} and sulphate peak shift is also observed in 1610-620 cm^{-1} spectral region towards larger values which correspond to the sulphate group fluctuations. Comparison IR spectra of all SAGs, a similar pattern is observed for SAG-2, SAG-4 and SAG-6, while in the area of 1240-1260 cm^{-1} the greater intensity bands are observed for SAG-2,4 in comparison with the SAG-2, SAG-4, and SAG-6.

a)

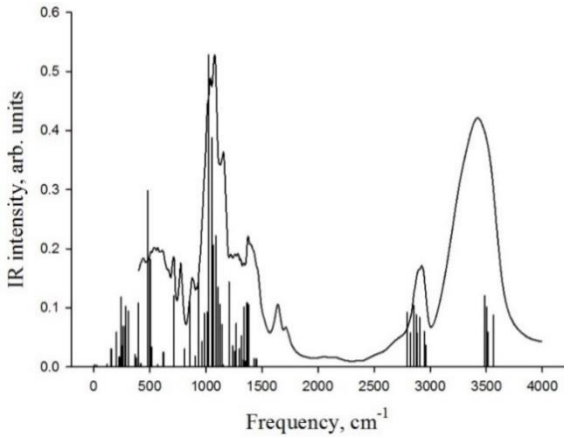

b)

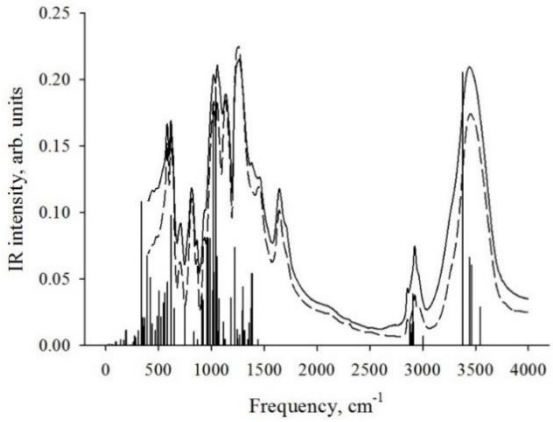

c)

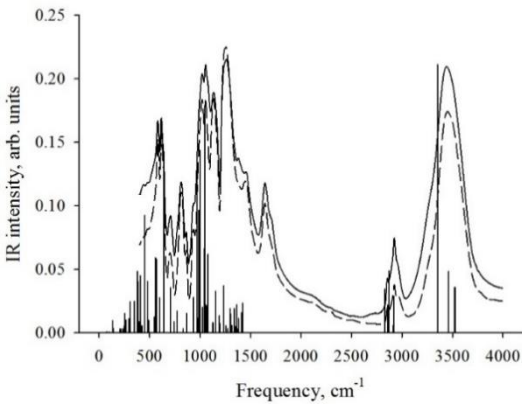

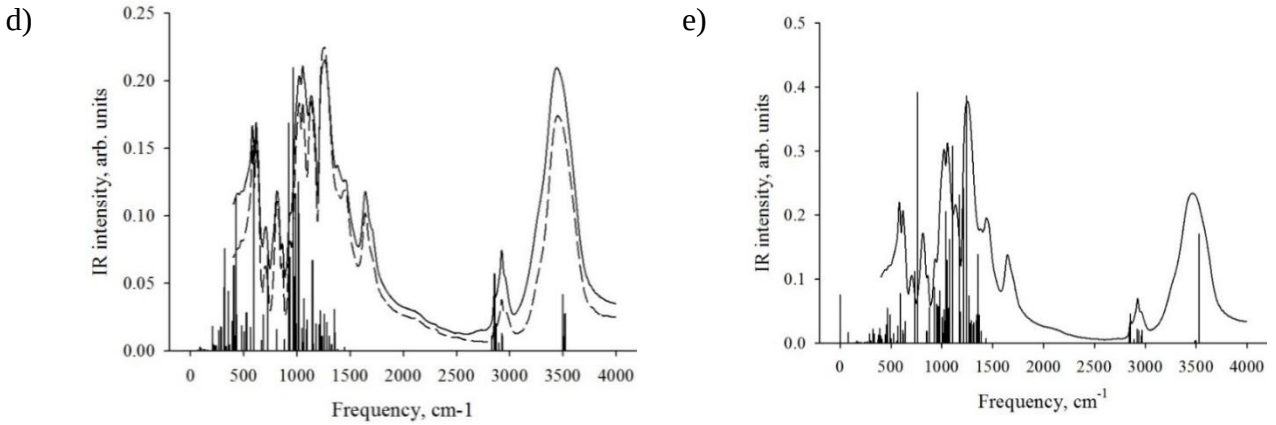

Figure 2. Experimental and theoretical IR spectra of arabinogalactan and its sulphated derivatives. Theoretical IR spectra at the B3LYP/6-31+G(d) level of theory are presented as vertical lines, while experimental IR countors are presented as black solid and dashed lines. a) Experimental and theoretical IR spectra of arabinogalactan. b) SAG-2 experimental and theoretical IR spectra. The solid line corresponds to 3.2% and the dashed line corresponds to 5.1% of sulphur content, respectively. c) SAG-4 experimental and theoretical IR spectra. The solid line corresponds to 3.2% and the dashed line corresponds to 5.1% of sulphur content, respectively. d) SAG-6 experimental and theoretical IR spectra. The solid line corresponds to 3.2% and the dashed line corresponds to 5.1% of sulphur content, respectively. e) SAG-2, 4 (9.4% of sulphur content, solid line) experimental and theoretical IR spectral.

Experimental (with mass sulphur content of 3.2% and 5.1%) and theoretical IR spectra of arabinogalactan and its sulphated derivatives (SAG-2, SAG-4, SAG-6, and SAG-2, 4) are presented in Figure 2. It is observed that the theoretical and experimental spectral corresponds well within 3000–4000 cm^{-1} spectral region.

Table 2 Theoretical (B3LYP/6-31+G(d) level of theory) and experimental absorption frequencies of -OH, $-CH_2$, $-SO_2$ functional groups of SAG-2, SAG-4, SAG-6, and SAG-2,4.

№	Ex. data	Calculated values								Band assignment*
		SAG-2		SAG-4		SAG-2,4		SAG-6		
	AF**, cm^{-1}	AF, cm^{-1}	RE, %	AF, cm^{-1}	RE, %	AF, cm^{-1}	RE, %	AF, cm^{-1}	RE, %	
1	2	3	4	5	6	7	8	9	10	11
2	581	540	7.59	550	5.34	504	13.25	580	0.17	$\delta_{(O=S=O)}$, $\delta_{(R-OH)}$
3	617	633	2.53	640	3.59	682	9.53	674	9.24	$\delta_{(R-OH)}$
4	710	782	9.21	778	8.74	774	8.27	760	7.04	$\delta_{(R-OH)}$, $\delta_{(-CH_2-)}$
5	934	927	0.75	933	0.11	950	1.68	991	6.10	$\delta_{(OH)}$, $\upsilon_{(C-O)}$, $\rho_{(CH_2)}$
6	1019	1013	0.59	995	2.36	1006	1.28	1074	5.40	$\delta_{(OH)}$, $\upsilon_{(C-O)}$, $\rho_{(CH_2)}$, $\upsilon_{s(O=S=O)}$

7	1131	1096	3.09	1095	3.18	1082	4.33	1206	6.63	$\tau_{(CH_2)}$, $\delta_{(OH)}$, $\upsilon_{(C-O)}$, $\delta_{(C-O-C)}$
8	1258	1264	0.47	1233	1.99	1274	1.26	1223	2.78	$\omega_{(CH_2)}$, $\upsilon_{(C-O)}$, $\delta_{(OH)}$, $\upsilon_{as(O=S=O)}$
9	1446	1435	0.76	1427	1.31	1452	0.41	1413	2.28	$\delta_{(-CH_2-)}$
10	2923	3038	3.79	3048	4.10	3051	4.20	3006	2.84	$\upsilon_{(CH_2)}$
11	3440	3656	5.91	3531	2.58	3705	7.70	3497	1.66	$\upsilon_{(OH)}$
average value		3.47		3.33		5.19		4.42		

SAG-2 refers to sulphated arabinogalactan with sulphate group located in C2 position;
SAG-4 refers to sulphated arabinogalactan with sulphate group located in C4 position;
SAG-2,4 refers to sulphated arabinogalactan with sulphate groups located in C2 and C4 positions;
SAG-6 refers to sulphated arabinogalactan with sulphate group located in C6 position.

* The following notations are used: ν is stretching vibration, δ, ρ, ω, τ are bending scissoring, rocking, wagging, and twisting vibrations.

** AF is absorption frequency, and RE is relative error ($RE=(AF_{exp}-AF_{theor})\cdot 100\%/ AF_{exp}$). Determination of spectral bands according to reference (Babkin et al. 2016).

According to Table 2, SAG-2,4 showed visible discrepancy up to 10% between theoretical and experimental results, which is probably due to the fact that the experimental samples contain sulphated polysaccharide galactose units with a different hydroxyl group sulphation degree in various polysaccharide monomeric structures in C2, C4, and C6 positions (Figure 1). It leads to widening and energy shift of experimental IR peaks which correspond to OH- and -CH_2- bonds in polysaccharide molecule.

Molecular structures of arabinogalactan and sulphated arabinogalactan (SAG-2,4) are presented in Figure 3, left and right, respectively, with chains consist of two galactose, arabinogalactan and sulphated units in 2,4 AG positions.

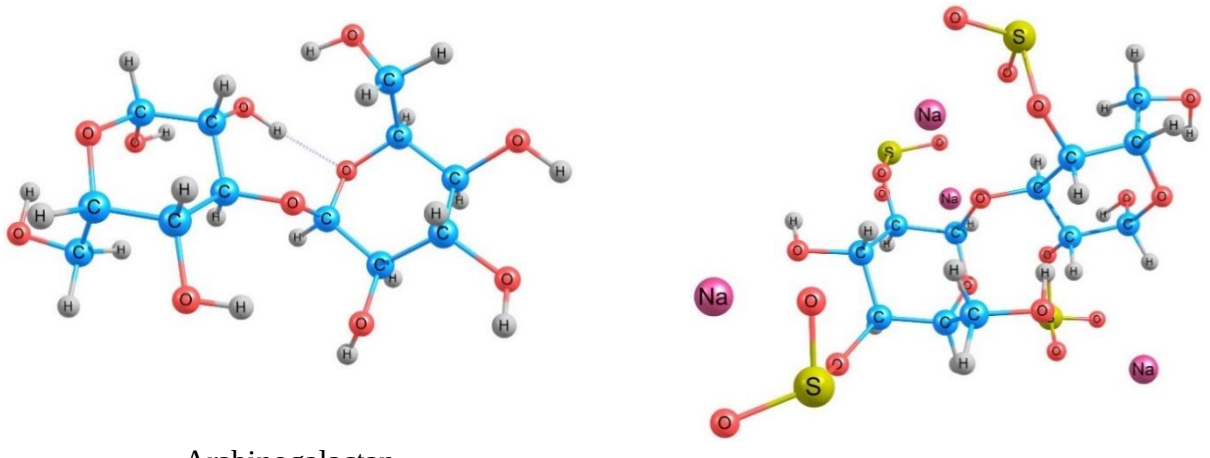

Arabinogalactan

Sulphated arabinogalactan

Figure 3. Molecular structure of galactose units of arabinogalactan and sulphated arabinogalactan in 2,4 position calculated at B3LYP/6-31+G(d) level of theory.

AG and SAG-2,4 IR spectra are presented in Figure 4. A band of 1690 cm^{-1} refers to the H-bond between two adjacent galactose units, which constitute AG and SAG molecules. It can be assumed that the intensity of intermolecular IR bands linearly increases with increasing of chain length, which may bring the theoretical spectrum closer to the experimental one with rather intense absorption bands in the of 1650-1750 cm^{-1} energy region (see for comparison Figure 2).

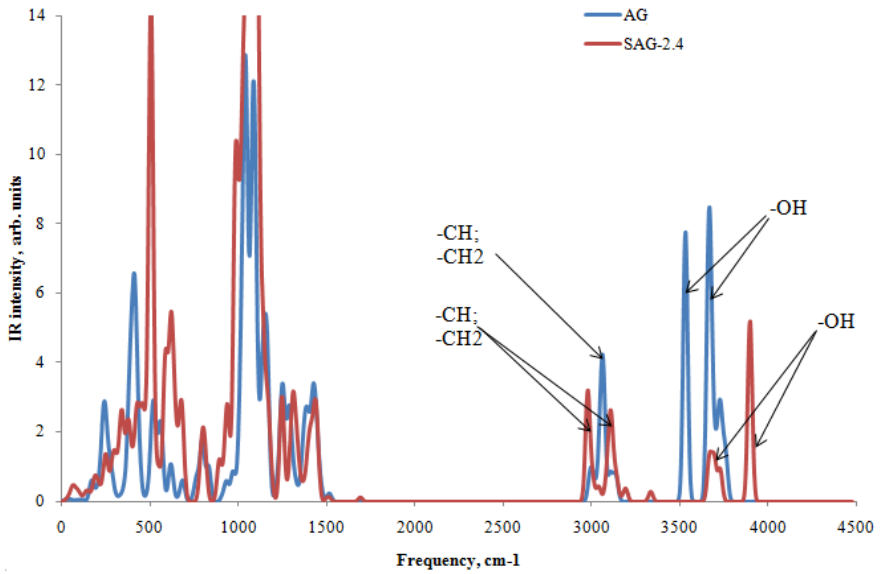

Figure 4. Theoretical B3LYP/6-31+G(d) IR spectra of arabinogalactan and sulphated AG in the 2,4 position, consisting of two galactose units. The red line represents IR spectrum of SAG-2,4, and blue one represents IR spectrum of arabinogalactan constituted of two monosaccharide units.

Table 3 presents theoretical vibration frequency assignments for functional groups in parent arabinogalactan and SAG-2,4, consisting of two galactose units.

Table 3 Theoretical vibration frequenciy assignment for the functional groups in arabinogalactan and SAG-2,4, both consisting of two galactose units.

AG oscillation frequencies		SAG-2,4 oscillation frequencies	
Oscillation frequency	Band assignment	Oscillation frequency	Band assignment
2993.31 3009.84 3035.94 3044.91	-CH	2977.77 3003.83 3036.94 3044.11	-CH
3051.1 3053.07 3061.97 3063.31 3066.17 3067.86	-CH, $-CH_2$	3084.91	$-CH_2$
3106.71 3109.68	-CH	3104.27 3109.96	-CH
3134.9 3144.93	-CH, $-CH_2$	3110.42 3117.71	-CH, $-CH_2$

		3132.01 3139.68 3170.1 3192.49	
-	-	3334.64	-CH
3533.57 3664.77 3678.15 3701.51 3724.01 3726.96 3739.82 3761.4	-OH	3667.22 3693.84 3727.1 3896.84	-OH

Comparison of the bond lengths and angles in arabinogalactan monomer and its sulphated derivatives

Theoretical bond lengths and bond angles of arabinogalactan monomer and its derivatives sulphated to different positions are presented in Figure 5 and Table 4.

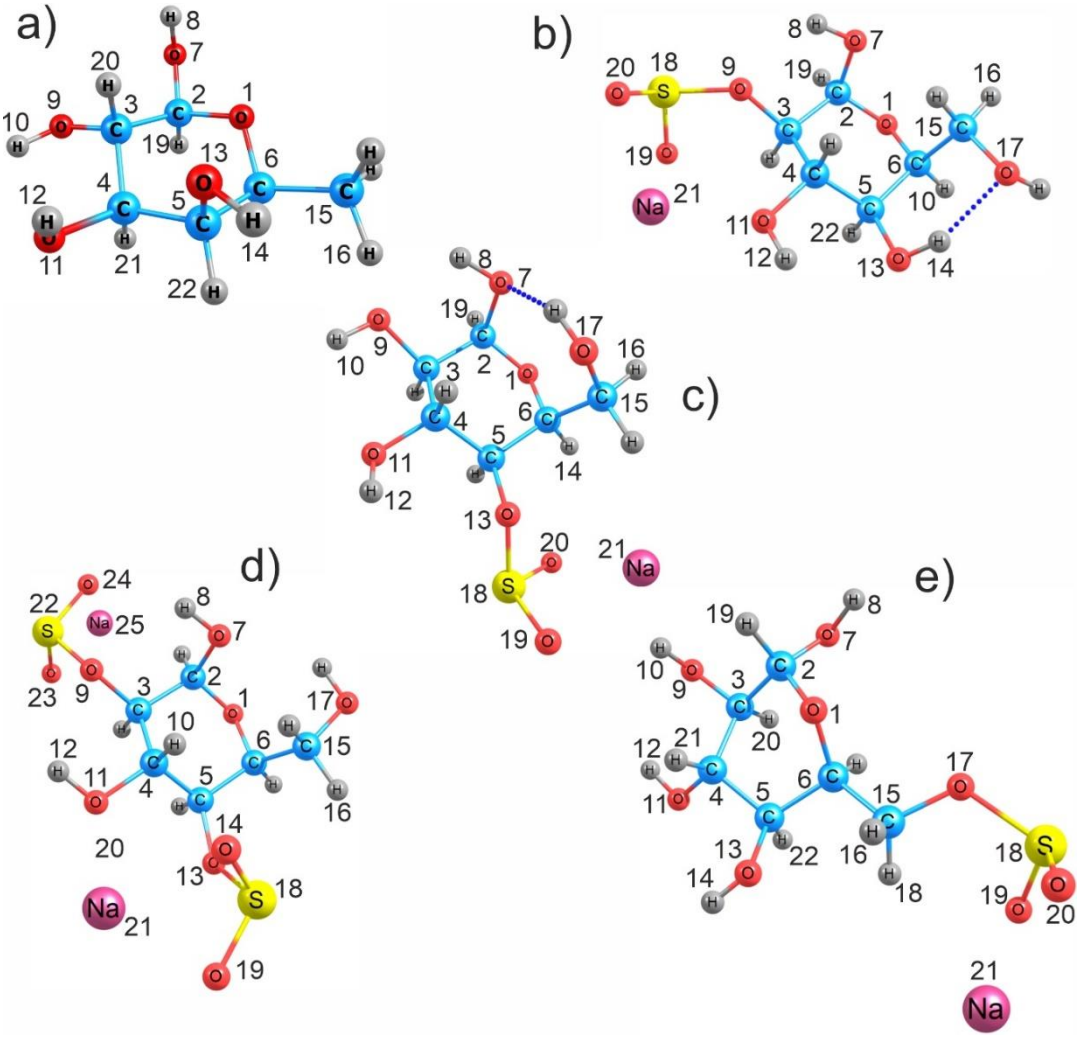

Figure 5. Molecular structure of AG and SAGs calculated at the B3LYP/6-31+G(d) level of theory. a) Parent arabinogalactane, b) SAG-2, c) SAG-4, d) SAG-2,4, e) SAG-6. The blue dotted lines represent intramolecular hydrogen bonds. Atoms are numbered following Table 4 notations.

Following decreasing of absorption energy E_{abs} (Table S1), it can be concluded that substitution of hydroxyl group of parent arabinogalactan by sulphate group should lead to increase of reactivity of its sulphated derivatives. With the addition of a sulphate group into the arabinogalactan structure, the hydroxyl groups become more accessible for further sulphation. The structural transformations can be caused by both structural breakdown during arabinogalactan sulphation (Vasilyeva et al. 2013) and differences in the conformation of the sulphated and parent polysaccharides. Obviously, sulphated arabinogalactan, unlike arabinogalactan, does not exist in spherical form.

Table 4. Bond lengths and angles of parent arabinogalactane, SAG-2, SAG-4, SAG-6, and SAG-2,4 molecules, calculated at B3LYP/6-31+G(d) level of theory. The details of the molecular structure are presented in Figure 5.

Atoms	AG	SAG-2	SAG-4	SAG-6	SAG-2,4
Bond lengths, Å					
O(1)-C(2)	1.42	1.41	1.40	1.42	1.40
C(2)-C(3)	1.54	1.55	1.54	1.54	1.54
C(3)-C(4)	1.54	1.53	1.53	1.53	1.53
C(4)-C(5)	1.53	1.53	1.53	1.54	1.54
C(5)-C(6)	1.54	1.54	1.55	1.55	1.55
C(6)-O(1)	1.44	1.44	1.45	1.44	1.45
O(11)-H(12)	0.98	0.98	0.97	0.97	0.98
C(2)-O(7)	1.40	1.42	1.44	1.41	1.42
C(4)-O(11)	1.43	1.44	1.43	1.43	1.44
C(6)-C(15)	1.52	1.54	1.54	1.52	1.54
C(15)-H(16)	1.10	1.10	1.10	1.10	1.10
C(15)-O(17)	-	1.44	1.42	1.44	1.43
S(18)-O(20)	-	1.52	1.52	1.53	1.52
S(18)-O(19)	-	1.52	1.52	1.53	1.52
O(19)-Na(21)	-	2.35	2.35	2.30	2.34
S(22)-O(23)	-	-	-	-	1.53
S(22)-O(24)	-	-	-	-	1.53
O(24)-Na(25)	-	-	-	-	2.33
Angle values, °					
C(2)-O(1)-C(6)	114	119	120	113	119
C(2)-O(7)-H(8)	109	106	107	109	108
C(4)-O(11)-H(12)	107	107	108	108	106
O(19)-S(18)-O(20)	-	108	108	105	108

The decrease in the dipole moment (Table S1) of SAG-4 may be explained by molecular conformation in which the total dipole moment is less than the dipole moment of C–O-SO_3Na functional group. The electrophilicity increase relates to the introduction of an electron-withdrawing sulphate group.

Conclusions

In summary, the molecular and electronic structure and infrared spectra of arabinogalactan and its biological active sulphated derivatives were interpreted using DFT B3LYP/6-31+G(d) level of theory. The main experimental spectral features were assigned to specific chemical bond vibrations. It was found that molecular models based on isolated galactose and arabinose monomer units of arabinogalactan and its sulphated derivatives can be used for correct simulations of IR spectra in the entire spectral region of 4000-500 cm^{-1}. The difference between the frequencies of experimental and theoretical IR spectra of sulphated AG derivatives is greater than for the parent arabinogalactan due to the increase of the number of possible isomers and conformers. The discrepancy between theoretical and experimental IR spectra may be caused by the shortcomings of simple molecular models based on 1-2 galactose and arabinose structural units in comparison with real macromolecular structure, which is characterized by absence of regular composition and crystal.

Acknowledgements

The reported work was funded by RFBR and the government of Krasnoyarsk region according to the research project № 18-43-242003. The study was carried out using equipment of the Krasnoyarsk Regional Center of Research Equipment, Federal Research Center "Krasnoyarsk Science Center SB RAS". The authors are grateful to I.V. Korolkova for IR-spectra.

Compliance with ethical standards

Conflict of interest. The authors declare that they have no confict of interest.

References:

Akman F (2016) Spectroscopic investigation, HOMO–LUMO energies, natural bond orbital (NBO) analysis and thermodynamic properties of two-armed macroinitiator containing coumarin with DFT quantum chemical calculations. Canadian Journal of Physics. 94(6):583-593, https://doi.org/10.1139/cjp-2016-0041

Akman F, Kazachenko AS, Vasilyeva NYu, Malyar YuN (2020) Synthesis and characterization of starch sulfates obtained by the sulfamic acid-urea complex. Journal of Molecular Strucrure. https://doi.org/10.1016/j.molstruc.2020.127899

Akman F. (2017). Coumarin-based random copolymer. J of Therm Comp Mater, 31(6): 729–744. https://doi.org/10.1177/0892705717720253

Alban S, Schauerte A, Franz G (2002) Anticoagulant sulfated polysaccharides: Part I. Synthesis and structure-activity relationships of new pullulan sulfates. Carbohydr Polym 47(3):267-276. https://doi.org/10.1016/S0144-8617(01)00178-3

Antonova GF, Usov AI (1984) The structure of arabinogalactan of Siberian larch wood (Larix sibirica Ledeb.) Russ J Bioorg Chem 10(12):1664–1669.

Babkin VA, Neverova NA, Medvedeva EN, Fedorova TE, Levchuk AA (2016) Investigation of physicochemical properties of arabinogalactan of different larch species. Russ J Bioorg Chem 42(7):23. https://doi.org/10.1134/S1068162016070025

Barsberg S. (2010) Prediction of Vibrational Spectra of Polysaccharides—Simulated IR Spectrum of Cellulose Based on Density Functional Theory. J Phys Chem B 114:11703–11708. https://doi.org/10.1021/jp104213z

Becker CF, Guimarães JA, Mourão PAS., Verli H (2007) Conformation of sulfated galactan and sulfated fucan in aqueous solutions: Implications to their anticoagulant activities. J Mol Graphics and Modelling 26(1):391–399. https://doi.org/10.1016/j.jmgm.2007.01.008

Canales, A., Boos, I., Perkams, L., Karst, L., Luber, T., Karagiannis, T., … Jiménez-Barbero, J. (2017). Breaking the Limits in Analyzing Carbohydrate Recognition by NMR Spectroscopy: Resolving Branch-Selective Interaction of a Tetra-Antennary N -Glycan with Lectins. Angewandte Chemie International Edition, 56(47), 14987–14991. doi:10.1002/anie.201709130

Chaidedgumjorn A, Toyoda H, Woo ER, Lee KB, Kim YS, Toida T, Imanari T (2002) Effect of (1-3)- and (1-4)-linkages of fully sulfated polysacchrides on their anticoagulant activity. Carbohyd Res 337(10):925–933.

Curtiss LA, Raghavachari K, Redfern PC, Pople JA (1997) Assessment of Gaussian-2 and density functional theories for the computation of enthalpies of formation. J Chem. Phys. 106(3):1063–1068. https://doi.org/10.1063/1.473182

Curtiss LA, Redfern PC, Raghavachari K (2005) Assessment of Gaussian-3 and test set of experimental energies. J Chem. Phys. 123:124107–124119. https://doi.org/10.1063/1.2039080

Desai UR (2004) New antithrombin-based anticoagulants. Med Res Rev 24(2):151-181. https://doi.org/10.1002/med.10058

Drozd NN, Bannikova GE, Makarov VA, Varlamov VP (2006) Anticoagulant activity of sulfated polysaccharides. Russ J Experim Clin Pharmacol 69(6):51-60.

Duus JØ, Gotfredsen CH, Bock K (2000) Carbohydrate Structural Determination by NMR Spectroscopy: Modern Methods and Limitations. Chem. Rev. 100(12):4589-4614. https://doi.org/10.1021/cr990302n

Ellis R., Green E., Winlove C. P. Connect. Tissue Res., 2009, 50, 29–36.

Ermakova MF, Chistyakova AK, Shchukina LV, Pshenichnikova TA, Medvedeva EN, Neverova NA, Belovezhets LA, Babkin VA (2010) Effect of arabinogalactan isolated from Siberian larch on the baking value of soft wheat flour and bread quality. Russ J Bioorg Chem 36(7):951-956. https://doi.org/10.1134/S1068162010070277

Fredj D, Hassen CB, Elleuch S, Feki H, Boudjada NC, Mhiri T, Boujelbene M (2017) Structural, vibrational and optical properties of a new organic-inorganic material: (C5H8N3)2[BiCl5], J. Mater. Res. Bull. 85:23–29. https://doi.org/10.1016/j.materresbull.2016.08.041

Garnjanagoonchorn W., Wongekalak L., Engkagul A. Chem. Eng. Process. Process Intensif., 2007, 46, 465–471

Gerbst AG, Nikolaev AV, Yashunsky DV. et al. Theoretical and NMR-based Conformational Analysis of Phosphodiester-linked Disaccharides. Sci Rep 7, 8934 (2017). https://doi.org/10.1038/s41598-017-09055-x

Goellner EM, Utermoehlen J, Kramer R, Classen B (2011) Structure of arabinogalactan from Larix laricina and its reactivity with antibodies directed against type-II-arabinogalactans. Carbohydr Polym 86(4):1739–1744. https://doi.org/10.1016/j.carbpol.2011.07.006

Huang H, Zhang W-D (2010) Preparation of Cellulose Sulphate and Evaluation of its Properties. J Fiber Bioeng Informat 3(1):32-39. https://doi.org/10.3993/jfbi06201006

Huang X, Hu Y, Zhao X, Lu Y, Wang J, Zhang F, Sun J (2008) Sulfated modification can enhance the adjuvant activity of astragalus polysaccharide for ND vaccine. Carbohydr Polym 73(2):303-308. https://doi.org/10.1016/j.carbpol.2007.11.032

Huang X, Wang D, Hu Y, Lu Y, Guo Z, Kong X, Sun J (2008) Effect of sulfated astragalus polysaccharide on cellular infectivity of infectious bursal disease virus. Intern J Biol Macromol 42(2):166-171. https://doi.org/10.1016/j.ijbiomac.2007.10.019

Jiao G, Yu G, Zhang J, Ewart S (2011) Chemical Structures and Bioactivities of Sulfated Polysaccharides from Marine Algae. Mar Drugs 9(2):196-223. https://doi.org/10.3390/md9020196

Karacsonyi S, Kovacik V, Alfoldi J, Kubackova M (1984) Chemical and 13C-NMR studies of an arabinogalactan from Larix sibirica L. Carbohydr Res 134(2):265–274. https://doi.org/10.1016/0008-6215(84)85042-9

Klepach T, Zhao H, Hu X, Zhang W, Stenutz R, Hadad MJ, Carmichael I, Serianni AS (2015) Informing saccharide structural NMR studies with density functional theory calculations. Methods Mol Biol. 1273:289-331. doi: 10.1007/978-1-4939-2343-4_20.

Kostiro JaA, Kovalskaja GN (2008) Sulphated arabinogalactan is a perspective domestically produced analog of sulodecside. Acta biomedica scientifica (2):117-119.

Lee C, Yang W, Parr RG (1988) Development of the Colle-Salvetti correlation-energy formula into a functional of the electron density. Phys Rev B 37:785. https://doi.org/10.1103/PhysRevB.37.785

Ma X, Guo Z, Wang D, Hu Y, Shen Z (2010) Effects of sulfated polysaccharides and their prescriptions on immune response of ND vaccine in chicken. Carbohydr Polym 82(1):9-13. https://doi.org/10.1016/j.carbpol.2010.04.013

Mainreck N., Brézillon S., Sockalingum G. D., Maquart F. X., Manfait M., Wegrowski Y., J. Pharm. Sci., 2011, 100, 441–450.

Matsuo K., Namatame H., Taniguchi M., Gekko K. Biosci. Biotechnol. Biochem., 2009, 73, 557–561.

Mestechkina NM, Shcherbukhin VD (2010) Sulfated polysaccharides and their anticoagulant activity: A review. Appl Biochem Microbiol 46(3):291-298. https://doi.org/10.1134/S000368381003004X

Nader HB, Lopes CC, Rocha HA, Santos EA, Dietrich CP (2004) Heparins and heparinoids: occurrence, structure and mechanism of antithrombotic and hemorrhagic activities.Curr Pharm Des 10(9):951–966. https://doi.org/10.2174/1381612043452758

Palivec V., Kopecký V., Jungwirth P., Bouř P., Kaminský J., Martinez-Seara H. (2019) Simulation of Raman and Raman optical activity of saccharides in solution. Physical Chemistry Chemical Physics. 2020, 22, 1983-1993. https://doi.org/10.1039/C9CP05682C

Pereira L, Amado AM, Critchley AT, Velde F, Ribeiro-Claro PJA (2009) Identification of selected seaweed polysaccharides (phycocolloids) by vibrational spectroscopy (FTIR-ATR and FT-Raman). Food Hydrocoll 23(7):1903-1909. https://doi.org/10.1016/j.foodhyd.2008.11.014

Pereira MS, Melo FR, Mourão PAS. (2002) Is there a correlation between structure and anticoagulant action of sulfated galactans and sulfated fucans? Glycobiology 12(10):573-580. https://doi.org/10.1093/glycob/cwf077

Profant V, Johannessen C, Blanch EW, Bour P, Baumruk V (2019) Effects of Sulfation and Environment on Structure of Chodroitin Sulfate Studied by Raman Optical Activity Phys. Chem. Chem. Phys. DOI: 10.1039/C9CP00472F.

Rudd T. R., Skidmore M. A., Guimond S. E., Cosentino C., Torri G., Fernig D. G., Lauder R. M., M. Guerrini, E. A. Yates, Glycobiology, 2009, 19, 52–67.

Rüther, A., Forget, A., Roy, A., Carballo, C., Mießmer, F., Dukor, R. K., L.A. Nafie, C. Johannessen, V. Prasad Shastri, Lüdeke, S. (2017). Unravelling a Direct Role for Polysaccharide β-Strands in the Higher Order Structure of Physical Hydrogels. Angewandte Chemie, 129(16), 4674–4678. doi:10.1002/ange.201701019

Shanura Fernando IP, Asanka Sanjeewa KK, Samarakoon KW, Lee WW, Kim H-S, Kim E-A, Gunasekara UKDSS, Abeytunga DTU, Nanayakkara C, de Silva ED, Lee H-S, Jeon Y-J (2017) FTIR characterization and antioxidant activity of water soluble crude polysaccharides of Sri Lankan marine algae. Algae 32(1):75-86. https://doi.org/10.4490/algae.2017.32.12.1

Shklyaev OE, Kubicki JD, Watts HD, Crespi VH (2014). Constraints on Ib cellulose twist from DFT calculations of 13C NMR chemical shifts. Cellulose, 21(6), 3979–3991. doi:10.1007/s10570-014-0448-3

Shmidt MW, Baldridge KK, Boatz JA, Elbert ST, Gordon MS, Jensen JH, Koseki S, Matsunaga N, Nguyen KA, Su SJ, Windus TL, Dupuis M, Montgomery JA (1993) General atomic and molecular electronic structure system. J Comp Chem 14:1347. https://doi.org/10.1002/jcc.540141112

Stewart JJ (2004) Optimization of parameters for semiempirical methods IV: extension of MNDO, AM1, and PM3 to more main group elements. J Mol Model 10(2):155-164. https://doi.org/10.1007/s00894-004-0183-z

Tirado-Rives J, Jorgensen WL (2008) Performance of B3LYP density functional methods for a large set of organic molecules. J Chem. Theory Comput. 4:297–306. https://doi.org/10.1021/ct700248k

Tran TTV, Huy BT, Truong HB, Bui ML, Thanh TTT, Dao DQ (2018) Structure analysis of sulfated polysaccharides extracted from green seaweed Ulva lactuca: experimental and density functional theory studies. Monatsh Chem 149: 197–205. https://doi.org/10.1007/s00706-017-2056-z

Vasil'eva NYu, Levdansky AV, Kuznetsov BN, Skvortsova GP, Kazachenko AS, Djakovitch L, Pinel C (2015) Sulfation of arabinogalactan by sulfamic acid in dioxane. Russ J Bioorg Chem 41(7):725–731. https://doi.org/10.1134/S1068162015070158

Vasilyeva NYu, Levdansky AV, Kazachenko AS, Djakovitch L, Pinel C, Kuznetsov BN (2013) Sulfation of Mechanically Activated Arabinogalactan by Complex Sulfuric Anhydride – Pyridine in Pyridine Medium. J Sib Fed Univ. Chem 6(2):158-169.

Willför S, Holmbom B (2004) Isolation and characterisation of water soluble polysaccharides from Norway spruce and Scots pine. Wood Sci Technol 38(3):173-179. https://doi.org/10.1007/s00226-003-0200-x

Yaffe, N. R., Almond, A., & Blanch, E. W. (2010). A New Route to Carbohydrate Secondary and Tertiary Structure Using Raman Spectroscopy and Raman Optical Activity. Journal of the American Chemical Society, 132(31), 10654–10655. doi:10.1021/ja104077n

Zhang H, Wang Z-Y, Yang L, Yang X, Wang X, Zhang Z (2011) In vitro antioxidant activities of sulfated derivatives of polysaccharides extracted from Auricularia auricular. Int J Mol Sci 12(5):3288-3302. https://doi.org/10.3390/ijms12053288.

Zhang K, Brendler E, Fischer S (2010) FT Raman investigation of sodium cellulose sulfate Cellulose 17(2):427–435. https://doi.org/10.1007/s10570-009-9375-0